

PCCP

Accepted Manuscript



This is an *Accepted Manuscript*, which has been through the Royal Society of Chemistry peer review process and has been accepted for publication.

Accepted Manuscripts are published online shortly after acceptance, before technical editing, formatting and proof reading. Using this free service, authors can make their results available to the community, in citable form, before we publish the edited article. We will replace this *Accepted Manuscript* with the edited and formatted *Advance Article* as soon as it is available.

You can find more information about *Accepted Manuscripts* in the [Information for Authors](#).

Please note that technical editing may introduce minor changes to the text and/or graphics, which may alter content. The journal's standard [Terms & Conditions](#) and the [Ethical guidelines](#) still apply. In no event shall the Royal Society of Chemistry be held responsible for any errors or omissions in this *Accepted Manuscript* or any consequences arising from the use of any information it contains.

Spin-Resolved NOCV Analysis of the Zeolite Framework Influence on The Interaction of NO with Cu(I/II) Sites in Zeolites[†]

Paweł Kozyra,^{*a} Witold Piskorz^a

Received Xth XXXXXXXXXXXX 20XX, Accepted Xth XXXXXXXXXXXX 20XX

First published on the web Xth XXXXXXXXXXXX 200X

DOI: 10.1039/b000000x

In the present work the function of zeolite framework in modifying the properties of copper sites has been studied. The $[\text{Al}(\text{OH})_4\text{CuNO}]^{0/+}$ systems were studied by applying the analysis of the electron density flows – contributions to deformation density between two interacting fragments. The systems were divided in the following partition scheme: the first fragment, $[\text{Al}(\text{OH})_4]^-$ (tagged T1), and the second one, $[\text{CuNO}]^{+/2+}$. The analysis allowed to elucidate the function of the zeolite fragment in modification of the cation properties towards activating the NO molecule. For both $[(\text{T1})\text{CuNO}]^{0/+}$ systems several channels showing the role of zeolite framework have been identified. The geometry of the adducts influence either the efficiency of the channels or spin polarization. The two most important channels, zeolite-cation, influence the flow of electrons between the copper site and the antibonding NO orbitals. One channel favors π -backdonation in the plane perpendicular to the Cu-N-O plane while the other contribution influences π -backdonation in the C-N-O plane. The first one is found only in the system with copper(I) and it is essential for facilitating π -backdonation and activating the NO molecule. The second channel is spin sensitive for both copper(I) and copper(II) sites. In the case of the system with copper(I) the second channel favors π -backdonation while in the system containing copper(II) the direction of these flows is opposite for α and β electrons.

1 Introduction

Zeolite frameworks proved to be efficient hosts for catalytic sites for exposing them to the gas phase and also for modifying the properties of the active sites. For that reason zeolites are commercially used in catalytic reaction, *e.g.* acidic zeolites or mesoporous materials in cracking^{1–3} or promoted with transition metal cations in redox processes,^{4–6} like NO abatement, among many others.

NO is one of the nitrogen oxides which are environmentally harmful and highly abundant pollutants and as such should be eliminated from flue gases. Zeolites are one of the group of catalyst which are studied in this field.^{7–12}

The process of NO activation by copper(I) site in ZSM-5 has been, since its discovery by Iwamoto *et al.*,^{13–15} widely studied by experimentalists^{16–20} as well as via computational methods.^{21–30}

Exceptional activity of Cu(I) site towards NO decomposition raised scientists' hope and inspired theoreticians to describe, explain, and understand this phenomenon. The most commonly used observable which gives the information on the strength of the bond is the stretching frequency registered

by IR spectroscopy. Indeed, the spectrum of NO adsorbed on Cu(I) site in Cu-ZSM-5 exhibits red-shift by 67 cm^{-1} , while NO frequency upon adsorption on Cu(II) site increases by 29 cm^{-1} .²⁴ Copper is introduced into zeolite framework by ion-exchange using the solution of copper(II) salt. During thermal activation most of copper is reduced. As copper(II) is a precursor of copper(I) site and copper(II) is still present upon activation the latter was also studied in terms of its localization and activity.^{31,32}

Although copper(I) site exhibits activity towards NO decomposition, bare cations remain inactive.³³ Mechanism of decomposition of NO catalysed by copper sites in zeolite has been investigated and some transition state geometries were suggested.^{34,35} The cationic sites formed by embedding transition metal ions in zeolites are widely investigated as the sites activating small molecules, either inorganic or organic,³⁶ via two main processes: donation and backdonation of electron density.^{37,38}

The novell computational tools deliver methods to elucidate the channels which contribute to the interaction between the site and the molecule. The decomposition of the differential electron density for the system (*i.e.* the difference between electron density for the system and for non-interacting fragments) by natural orbitals for chemical valence (NOCV) into independent density transfer channels is useful and easy for interpretation. Such analysis has been performed for the interaction between silver and copper sites with ethene, ethyne,

[†] Electronic Supplementary Information (ESI) available: [details of any supplementary information available should be included here]. See DOI: 10.1039/b000000x/

^a ul. Ingardena 3, 30-060 Kraków, Poland. Fax: (++48) 126340515; Tel: (++48) 126632081; E-mail: kozyra@chemia.uj.edu.pl

* Corresponding author

formaldehyde,³⁹ benzene,⁴⁰ and NO molecule.^{41,42}

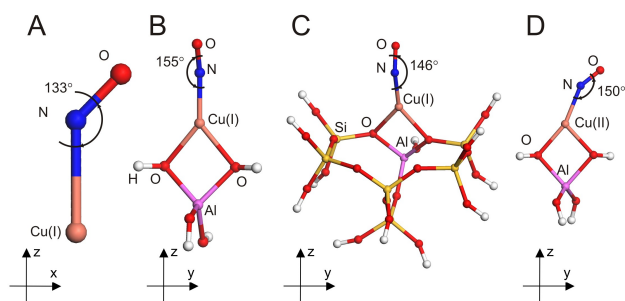


Fig. 1. Geometry optimized structures: $[\text{CuNO}]^+$ (A), $[(\text{T1})\text{CuNO}]$ (B), $[(\text{M7})\text{CuNO}]$ (C), $[(\text{T1})\text{CuNO}]^+$ (D) and orientation of the coordinates systems.

In this work the attention was focused on the function of the zeolite surrounding the Cu^+ and Cu^{2+} cations interacting with the NO molecule. The NOCV analysis was used to elucidate the influence of zeolite-cation electronic interaction (electron density donation/backdonation) on the cation-NO electron flows. The Fig. 1 shows the optimized structures of the models: $[\text{CuNO}]$, $[(\text{T1})\text{CuNO}]$, $[(\text{M7})\text{CuNO}]$, $[(\text{T1})\text{CuNO}]^+$. For Cu(I) models, the Cu-N-O plane is perpendicular to the plane of $\text{Al}(\text{O})_2\text{Cu}$, while for the models with Cu(II) the Cu-N-O is coplanar to it.

The complex form of the deformation density (see Computational details for definition) for $[\text{CuNO}]^+$ and $[(\text{T1})\text{CuNO}]^0$, shown in Fig. 2, justify the necessity of further partition analysis.

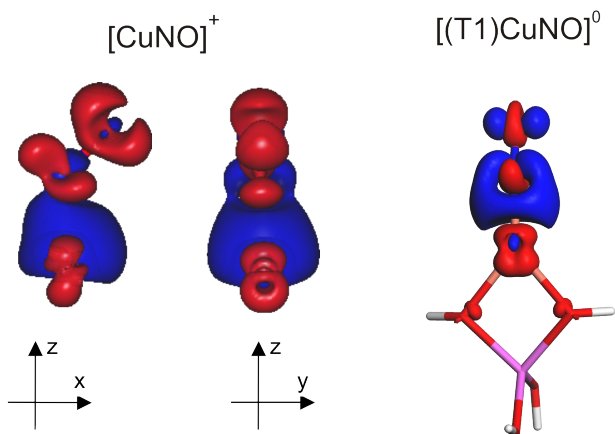


Fig. 2. Contour plots of overall deformation density for $[\text{CuNO}]^+$ and the $[(\text{T1})\text{CuNO}]^0$; red: electron outflow, blue: electron inflow, contour values: 0.004 a.u. and 0.002 a.u., respectively.

The most important electron density contributions transfer channels for the NO molecule interacting with bare copper, the

Cu^+ cation, or the copper(I) site have already been studied⁴¹ and the pivotal conclusions presented therein will be recalled here for the sake of clarity. As long as the zeolite framework is not included in the system, there are four contributions to differential density: (i) donation of unpaired α -electron from $\pi_{\parallel}^*(\text{NO})$ to d_{π} orbital of Cu^+ , (ii) π -backdonation from Cu^+ cation to NO molecule, (iii) covalent bond - donation to the bonding space, and (iv) σ -donation from NO molecule to *e.g.* orbital 4s on Cu^+ . The “ \bullet_{\parallel} ” and “ \bullet_{\perp} ” subscripts hereafter denote the orbitals with lobes parallel and perpendicular to Cu-N-O plane, respectively. First two contributions change significantly upon embedding the cation into the T1 fragment (see Fig. 3). The contribution (iii) which is a “covalent” donation from π_{\parallel} of NO remains almost unchanged. However, σ -donation from nitrogen lone pair (iv), not symmetric in α and β channels for CuNO^+ , becomes symmetric. Although such a small model as T1 cannot reproduce *e.g.* influence of different zeolite framework, the main contributions to the bonding between fragments hold and expanding T1 model to M7 hardly affects the differential density contributions (Table 2 in ref.⁴¹).

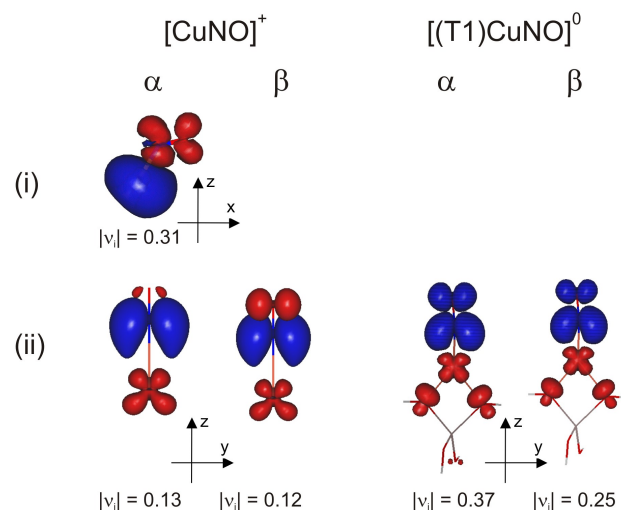


Fig. 3. Contour plots of dominant density transfer channels (for α and β densities) between bare Cu^+ (on the left) or (T1)Cu (on the right) and the NO molecule; red: electron outflow, blue: electron inflow, contour values: 0.001 a.u.

Deformation density for the interaction between two fragments of the $[(\text{T1})\text{CuNO}]^+$ system NO and $[(\text{T1})\text{Cu}]^+$ also has been decomposed into electron transfer channels using NOCV.⁴² Surprisingly, they resemble those obtained for NO and $[(\text{T1})\text{Cu}]$. Because of symmetry the strong interaction is allowed between π_{\parallel}^* of NO and $d_{\pi_{\parallel}}$ orbital of copper(II) cation. Again, the donation of unpaired α electron from NO molecule to copper cation (i) has the highest eigenvalue (0.50).

The π -backdonation (ii) from the cation to NO molecule occurs in both α and β channels but is less efficient than for $[(\text{T1})\text{CuNO}]^0$. “Covalent” donation from π_{\parallel} of NO to copper (iii) and σ -donation from the nitrogen lone pair (iv) are significant only in β channel as it was for the case of $[\text{CuNO}]^+$.

2 Computational details

The computational details were consistent with our previous work.⁴² We performed calculation with the Turbomole package⁴³ with def2-TZVP⁴⁴ basis set and DFT level of theory with PBE0 functional.⁴⁵ Our models are composed of a single aluminate tetrahedron T1, $[\text{Al}(\text{OH})_4]^-$, a copper cation Cu^+ or Cu^{2+} , and NO. The ground state of $[(\text{T1})\text{CuNO}]^0$ was doublet. The promolecules in this case were singlet T1 and doublet $[\text{CuNO}]^+$. The ground state of $[(\text{T1})\text{CuNO}]^+$ was an open-shell singlet, however both T1 and $[\text{CuNO}]^{2+}$ turned out to be the closed-shell systems. All the molecules and promolecules were treated in spin-unrestricted formalism, also for NOCV analysis even for the closed-shell systems.

As Cu-N-O atoms are not collinear in both $[(\text{T1})\text{CuNO}]^0$ or $[(\text{T1})\text{CuNO}]^+$ the orbitals of $[\text{CuNO}]^{+/2+}$ fragments are oriented unambiguously. We denote antibonding orbitals of NO depending on the orientation to the Cu-N-O plane: one is in plane (π_{\parallel}^*), while the other is perpendicular (π_{\perp}^*). Taking into account that NO, NOCu^+ , and Cu(II) site are open-shell systems, it was necessary to perform the unrestricted calculation. Surprisingly, while Cu(II) cation is not affected by zeolite, the promolecule CuNO^{2+} is a closed-shell system. The stability of the electronic structure was verified by the *escf* module (Turbomole).⁴⁶

Because the restricted Hartree-Fock (RHF) or the restricted Kohn-Sham (RKS) formalisms guarantee the desired spin and symmetry properties during electronic structure optimization, which causes that the (local) stability should be rather regarded as the metastability, it is frequently desirable to verify the stability of the solution against the perturbations which could break spin or spatial symmetry. In the *escf* tool the stability analysis is performed via the second order variation of the occupied orbitals. It allows for the determination whether the stationary point, obtained by the electronic structure optimization, is a real minimum or rather the saddle point. It can also be determined whether such variation breaks the spatial/spin symmetry of the restricted (RHF/RKS) solutions.

Deformation density, $\Delta\rho$, is defined as the difference between the electron density for the system and fragments. The density for the fragments are calculated adiabatically, i.e. in the geometry suitable for the system but without interaction between them. Hence, the deformation density stores the information on the interaction between the fragments. For the sake of clear interpretation the overall deformation density can

be decomposed by using NOCV analysis.

The natural orbitals for chemical valence (NOCV) theory is based on the differential (deformation) electronic density defined as the difference between the molecular density and the sum of the densities for atoms (generally: fragments). Hence, its positive sign denotes the accumulation of the charge while the negative sign means depletion. The NOCVs diagonalize the deformation density matrix defined as $\Delta\mathbf{P} = \mathbf{P} - \mathbf{P}_0$, where \mathbf{P} and \mathbf{P}_0 denote density matrices for combined molecule and molecular fragments, respectively. The deformation density can also be decomposed into NOCVs. Such eigenvectors denote the electron density flow channels, namely donation and back-donation. NOCV eigenvalues (v_k) represent the difference of occupation for pairs of coupled NOCVs with respect to the state of non-interacting promolecules thus the meaning of v_k is the number of electron transferred in the given channel.^{47–49}

Although the NOCV analysis is already implemented in e.g. SCM's ADF program we have used own-made program⁵⁰ for its maturity and flexibility – it performs post-processing of output from any quantum-chemical code capable of generating output files in molden format (Turbomole in this case).

3 Results and Discussion

3.1 NO interaction with Cu(I) site

As was said before, NO interacts with copper(I) site in the zeolite and the latter, forming the Cu^+ surrounding, is responsible for the modification of the properties of copper cation becoming the copper site. To elucidate such influence the NOCV analysis was made for the following partitioning scheme: one fragment was $[\text{CuNO}]^+$ and the other was T1 or M7. Four significant contributions appear in this scheme (Fig. 5). In both α and β channels the most important flows (with $|v_i| = 0.28$ and 0.24 , respectively) favors π -backdonation. Electron density diminishes on d_{π} (yz plane) orbitals of Cu^+ and p orbitals of oxygen atoms, and is transferred to the antibonding π_{\parallel}^* NO orbitals. This is the effect which is enhanced by T1 fragment and in such case the π -backdonation becomes much more efficient what is clearly seen in increase of NOCV eigenvalues for (ii) channels (Fig. 3): $|v_i|$ values change from $0.13/0.12$ to $0.37/0.25$. These perturbations weaken the N-O bond what reflects in the red-shift of IR spectra.³⁷ Enhancing π -backdonation additionally prevents NO from becoming positively charged. NO Mulliken charge is $+0.30$ for CuNO^+ system, while it is only 0.04 for $[(\text{T1})\text{CuNO}]^0$.

The most important channel (i), Fig. 3, with the highest $|v_i|$ value for $[\text{CuNO}]^+$ and present only for α electrons, disappears when T1 fragment is adjoined. The reason for this can be identified when analyzing T1/ $[\text{CuNO}]^+$ partition scheme.

The deformation densities for the interaction of T1 fragment

with either CuNO^+ or CuNO^{2+} are depicted in Fig. 4. Upon the interaction the T1 loses electrons while the positive fragments are being neutralized partially. The pictures are different for Cu(I) and Cu(II), however deeper insight into the interaction is hardly possible. That picture shows the results of at least a few contributions for α and β electrons so the apparent superimposition of a number of processes like donation, backdonation, polarization, or forming a covalent bond make the interpretation hardly possible. For these partition schemes we have made also the NOCV analysis which delivered more detailed information on the interaction between the fragments.

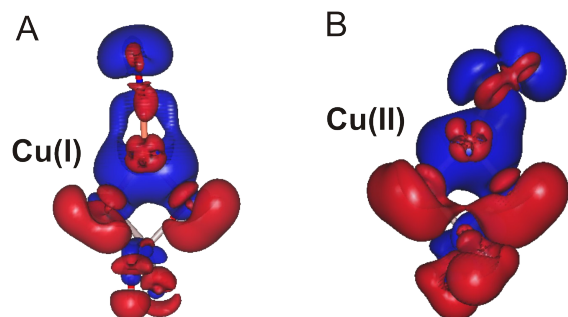


Fig. 4. Contour plots of overall differential density for the interaction between fragments T1^- and the CuNO^+ (A) and T1^- and the CuNO^{2+} (B); red: electron outflow, blue: electron inflow, contour values: 0.002 a.u.

NOCV contributions to deformation density were divided into two groups, depending on the spatial localization of the channels. Channels crucial for the interaction between cation and the admolecule were classified in the group A while those responsible for the interaction between cation and the framework are labeled with letter B. The A1 contribution (Fig. 5), appearing for α electrons, corresponds to the electron flow in the direction opposite to (i) channel, hence the α -A1 channel partially cancels out donation from antibonding NO orbital to the Cu^+ cation thus preventing from strengthening the N-O bond. In the other words, α -A1 contribution also increases activating ability of copper(I) site. This is also the reason for the spin density distribution (increase in NO molecule to the value of 1.03) which is shown in Fig. 6 (left panel).

The orientation, with respect to T1 fragment, of spin density lobes, parallel to the Cu-N-O plane, is different for Cu(I) and Cu(II) systems, while the spin density on NO is spatially distributed similarly (Fig. 6, right panel) despite the fact that $[(\text{T1})\text{CuNO}]^+$ is a singlet.

For CuNO^+ (Fig. 3 left panel) the flow of α electrons from unpaired NO orbital suppressed σ -donation from lone pair of nitrogen (iv) to Cu^+ in α channel (not shown here, see ref.⁴¹). Upon emerging of α -A1 flow for Cu(I) site and suppressing (i) channel σ -donation (iv) becomes symmetric in α and β channels.

In the β -B1 channel, the electron density gathers on the Cu(I) site at the expense of p orbitals of framework oxygen atoms to eventually neutralize both copper charge and copper spin density. The differential density has a few more contributions with eigenvalues 0.06-0.10 (not shown in the picture) representing mainly the interaction between oxygen atoms and the copper cation.

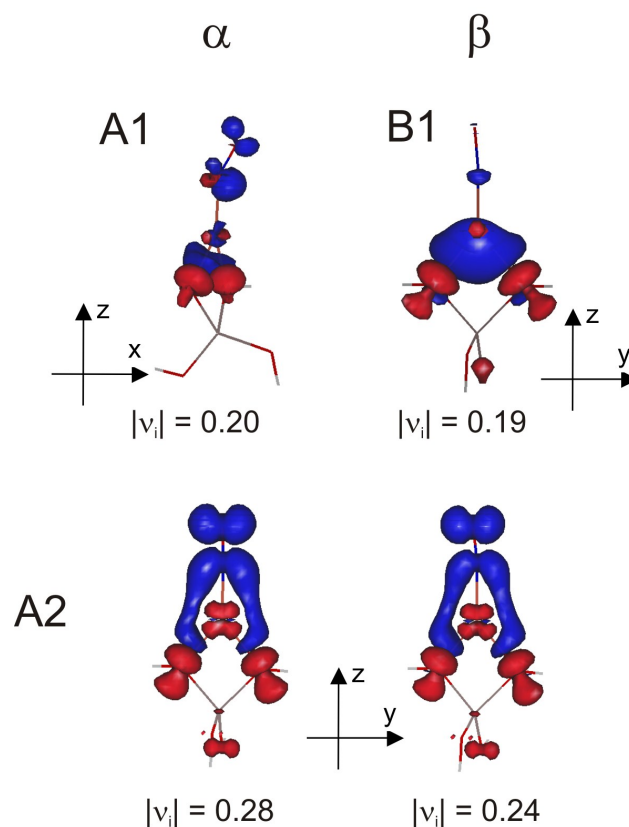


Fig. 5. Contour plots of dominant density transfer channels (for α and β densities) between T1 and the CuNO^+ fragment; red: electron outflow, blue: electron inflow, contour values: 0.001 a.u.

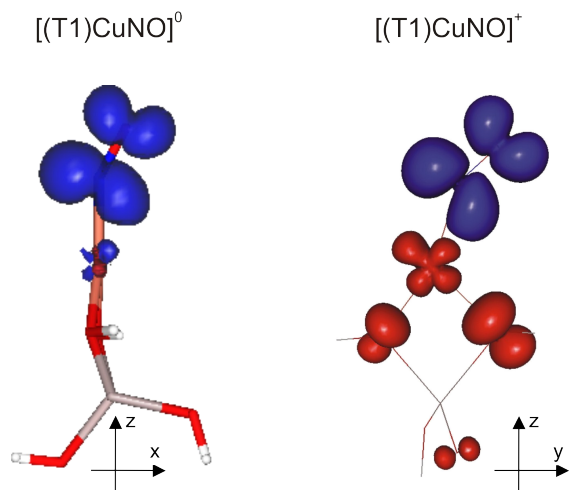


Fig. 6. Contour plot of the spin density (ρ_s) for doublet ground state of $[(T1)CuNO]^0$ and open-shell singlet $[(T1)CuNO]^+$, $|\rho_s| > 0.005$ a.u.; excess of spin α : blue, excess of spin β : red.

To verify the results obtained within the T1 model of zeolite framework, the smallest possible one, the calculations were also performed for an extended M7 model composed of six silica tetrahedra and one aluminum tetrahedron. The results are presented for the partition scheme analogous to that used previously, namely in which $CuNO^+$ is the 1st fragment and the zeolite framework M7 is the 2nd fragment. The results for spin-resolved NOCV analysis are presented in Fig. 7. The contributions to differential density with the highest eigenvalues are similar to those for (T1)CuNO model.

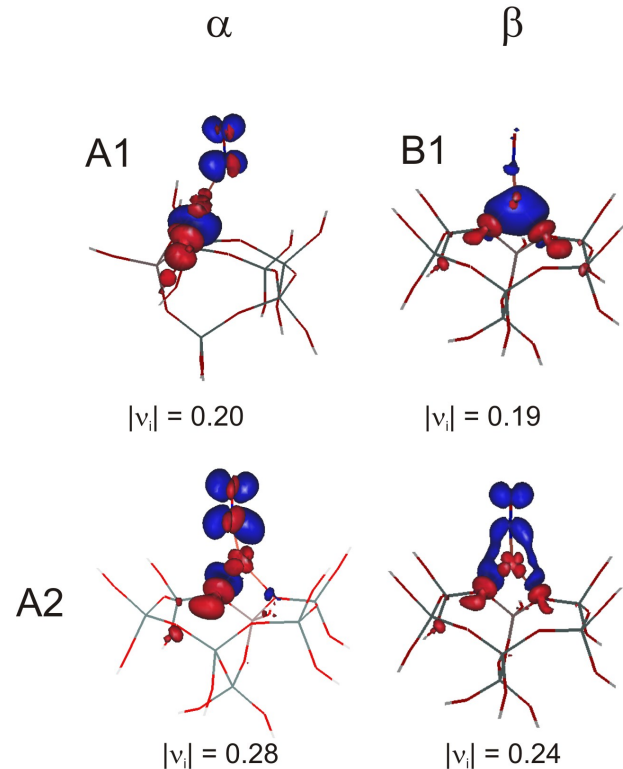


Fig. 7. Contour plots of dominant density transfer channels (for α and β densities) between M7 and the $CuNO^+$ molecule; red: electron outflow, blue: electron inflow, contour values: 0.001 a.u.

3.2 NO interaction with Cu(II) site

The interaction of NO with Cu(II) is similar to some extent to that for Cu(I). However, the NO group is rotated by 90° comparing to the case Cu(I) (now the Cu(II)-N-O fragment is in O-Al-O plane of the T1 fragment). For the NOCV analysis the $[(T1)CuNO]^+$ system was divided in the analogous way into two fragments: $(T1)^-$ and $[CuNO]^{2+}$. The charges of the fragments are ascribed on the basis of the formal oxidation state, in line with population analysis. For $[(T1)CuNO]$ the charge on CuNO fragment is +0.42, while for $[(T1)CuNO]^+$ the charge on CuNO is +0.97. Thus in the case of $[(T1)CuNO]^+$ the system was divided into $(T1)^-$ and $[CuNO]^{2+}$ – the former fragment was the same as in the case of $[(T1)CuNO]^0$ and holds more positive CuNO fragment.

The whole $[(T1)CuNO]^+$ system is an open-shell singlet while T1 and $CuNO^{2+}$ are closed-shell fragments. For the promolecule $[CuNO]^{2+}$ the stability analysis was performed with the use of *escf* module in Turbomole package which justified the closed-shell electronic structure of $[CuNO]^{2+}$. In the $[CuNO]^{2+}$ complex the ligand-to-metal charge transfer takes

place so the electronic structure is close to $[\text{Cu}^+-\text{NO}^+]$. Comparing the results for Cu(I) and Cu(II) the most striking is the absence of the A2 contribution favoring π -backdonation in the plane parallel to Cu-N-O which is most important in the case of Cu(I) site and crucial for NO activation.

Interaction between T1 and $[\text{CuNO}]^{2+}$ leads to breaking spin symmetry because NO α -antibonding orbital in the Cu-N-O plane (π_{\parallel}^*) is populated upon interaction (Fig. 8, A1). It can be discussed from two points of view. On one hand, α electron occupies antibonding orbital in NO before interacting with copper(II) site. The interaction leads to a weak antiferromagnetic coupling and some spin density remains on the NO molecule. The other part of spin density, $\sim 30\%$, is paired with β electrons from copper cation forming a weak covalent bond. Finally, some spin density remains on NO and some on T1 fragment forming the spin polarized system: the open-shell singlet. On the other hand, the $[\text{CuNO}]^{2+}$ fragment is a closed-shell system and the zeolite framework is spin-polarizing the system. Indeed, the reaction of the zeolite framework in the presence of $[\text{CuNO}]^{2+}$ is different in α and β channels — contour plots for NOCV analysis for interaction between T1 and the CuNO^{2+} are summarized in Fig. 8. The most important channel with eigenvalue of 0.76 (α -A1) has σ symmetry and can be interpreted (similarly to α -A1 for $[(\text{T1})\text{CuNO}]^0$, Fig. 5) as the donation opposing to that of unpaired electron from π_{\parallel}^* (A1) to Cu(II). However, taking into consideration that in this case the π_{\parallel}^* was unoccupied in the promolecule $[\text{CuNO}]^{2+}$, the A1 channel appears as a donation, only in α channel, what evokes spin polarization. In this channel electrons come from copper d orbital lying in yz plane and p orbitals of oxygen atoms. It can be clearly seen by decomposing the spin density into contributions expressed by spin NOCVs. The decomposition has been done by diagonalization of spin density matrix and finding the set of spin density NOCVs. By doing this, one pair of natural spin orbitals with eigenvalue of 0.76 has been obtained. These two spinorbitals (Fig. 9) reproduce spin density entirely. The contours show contributions which, squared, represent outflow ($v_i < 0$) and inflow ($v_i > 0$) of α electron density for the donation process from copper and oxygen atoms to the NO molecule.

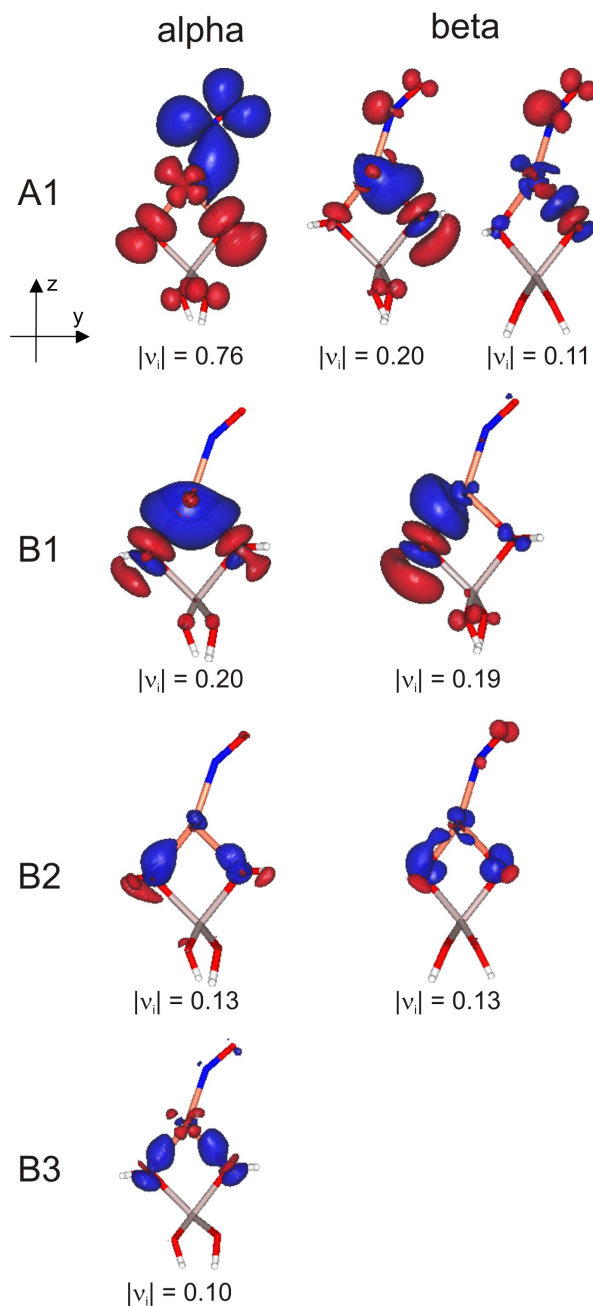


Fig. 8. Contour plots of dominant density transfer channels (for α and β densities) between T1 and the $[\text{CuNO}]^{2+}$ fragment; red: electron outflow, blue: electron inflow, contour values: 0.001 a.u.

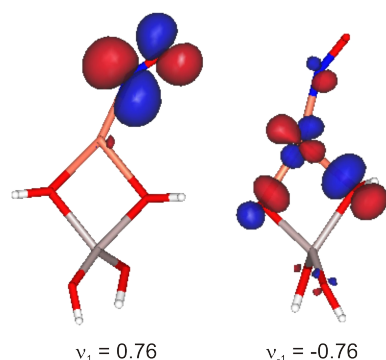


Fig. 9. Contour plots of the spin natural orbitals; contour value: 0.07 a.u.; left: inflow, right: outflow.

The α -A1 contribution is complementary to the (i) α electron contribution. In both partition schemes the electrons are transferred between α -antibonding spinorbital lying in the Cu-N-O plane ($\pi_{||}^*$) and the cation. The overall picture depends solely on the initial state which reflects the way of fragmentation since the resultant state is the same in both cases. Initially, in this partitioning scheme NO antibonding orbitals are unoccupied and upon the interaction with T1 fragment α electrons populate NO antibonding orbital. Two β -A1 contributions slightly enhance π -donation from NO and contain admixture of covalent bond between oxygen atoms and copper cation. The B1 contributions (α and β electrons) complement covalent Cu-O σ bonds in which orbital 4s is populated. The B2 contributions have π symmetry (yz nodal plane) in which d orbital on copper and p orbitals localized on oxygen atoms lying in xz plane take part. The last contribution (with eigenvalue > 0.10) to differential density, B3, corresponds to the σ -bonding between oxygen and copper but in this channel only d orbital (in yz plane) is engaged.

Actually, only one contribution (α -A1) is relevant here in the spin density, but others, although giving virtually no contribution to the spin density, give significant rise to the total electron density and hence are important for the interaction between cation and the zeolite framework.

4 Conclusions

In the present work the [(T1/M7)CuNO]^{0/+} systems have been studied by applying the partition scheme in which T1 (or M7) is one fragment and [CuNO]⁺ or [CuNO]²⁺ constitutes the second one. It allowed for elucidation the function of the zeolite fragment in the modification of the Cu-NO charge and spin interplay. For both [(T1)CuNO]⁰ or [(T1)CuNO]⁺ systems several channels have been identified and are gathered in Table 1.

Table 1. Descriptors and the character for independent electron transfer channels between fragments and corresponding spin-resolved eigenvalues (in arbitrary units) for models of [(T1)Cu(I)NO]⁰, [(M7)Cu(I)NO]⁰, [(T1)Cu(II)NO]⁺; labels *d* or *bd* indicate the donation and backdonation, respectively.

		[(T1)CuNO] ⁰	[(M7)CuNO] ⁰	[(T1)CuNO] ⁺
A1. Influencing π -backdonation in the C-N-O plane	α	0.23(<i>bd</i>)	0.22(<i>bd</i>)	0.76(<i>bd</i>)
	β	—	—	0.20 + 0.11(<i>d</i>)
A2. Supporting π -backdonation in the plane perpendicular to Cu-N-O	α	0.28	0.28	—
	β	0.24	0.24	—
B1. Covalent Cu-O interaction, σ contribution, 4s(Cu) engaged	α	*	*	0.20
	β	0.18	0.18	0.19*
B2. Covalent Cu-O interaction, π contribution	α	—	—	0.13
	β	—	—	0.13
B3. Covalent Cu-O interaction, σ contribution, d(Cu) engaged	α	< 0.1	< 0.1	0.10
	β	< 0.1	< 0.1	< 0.1

* A1 contributions have admixture of B1 contribution.

The oxidation state and geometry of the adducts influence the efficiency of the channels as well as spin polarization. The A1 and A2 channels are important for the interaction between the site and the NO molecule. They both influence the flow of electrons between the copper site and antibonding NO orbitals. The A1 contribution influences π -backdonation in the C-N-O plane while the channel A2 favors π -backdonation in the plane perpendicular to the Cu-N-O plane. The other channels (B1, B2, B3) represent interaction between the framework oxygens and the cation. The A1 channel is the one which is spin sensitive both for copper(I) and copper(II) sites. In the case of the system with copper(I) the A1 channel facilitates π -backdonation while in the system containing copper(II) the direction of the A1 flows is opposite — α electrons flow from the zeolite and the cation to the antibonding NO orbital. The A2 channel is found only in the system with copper(I) and it is essential for favoring π -backdonation and activating the NO molecule. Both A1 and A2 channels modulate the properties of the centers and the interaction with NO molecule. It is worth to notice that the framework modifies the properties of the cation but the interaction depends also on an adsorbed molecule which is integral and important part of NOCu⁺ and NOCu²⁺ fragments.

The most important finding of this work is the identification of the channel supporting π -backdonation which usually is crucial for the activating of adsorbed molecule and the channel evoking spin polarization. The spin resolved NOCV analysis with the proper partitioning scheme turned out to be a very powerful tool for the detailed look into the interaction between fragments of the system.

5 Acknowledgements

The authors gratefully acknowledge Prof. Ewa Brocławik, Dr. Mariusz Radoń, Mr. Adam Stepniewski, MSc, and Prof. Jerzy Datka for fruitful discussion as well as National Science Centre for the financial support (Grant No.: 2011/01/B/ST5/00915).

References

- V. Frilette, P. B. Weisz and R. L. Golden, *Journal of Catalysis*, 1962, **1**, 301–306.
- K. Tanabe and W. F. Hölderich, *Applied Catalysis A: General*, 1999, **181**, 399–434.
- Z. Zhang, Y. Han, L. Zhu, R. Wang, Y. Yu, S. Qiu, D. Zhao and F.-S. Xiao, *Angewandte Chemie International Edition*, 2001, **40**, 1258–1262.
- K. Klier, *Langmuir*, 1988, **4**, 13–25.
- A. Kanada, N. Idaka, S. Nishiyama, S. Tsuruya and M. Masai, *Phys. Chem. Chem. Phys.*, 1999, **1**, 373–381.
- P. Ratnasamy and D. Srinivas, *Catalysis Today*, 2009, **141**, 3–11.
- M. C. Campa, S. De Rossi, G. Ferraris and V. Indovina, *Applied Catalysis B: Environmental*, 1996, **8**, 315–331.
- M. Cristina Campa, *Applied Catalysis B: Environmental*, 1998, **18**, 151–162.
- J. L. D'Itri and W. M. H. Sachtler, *Catalysis Letters*, 1992, **15**, 289–295.
- T. V. Voskoboynikov, H.-Y. Chen and W. M. Sachtler, *Applied Catalysis B: Environmental*, 1998, **19**, 279–287.
- F. Kapteijn, J. Rodriguez-Mirasol and J. A. Moulijn, *Appl. Catal. B*, 1996, **9**, 25.
- A. Heyden, B. Peters, A. T. Bell and F. J. Keil, *J. Phys. Chem. B*, 2005, **109**, 1857.
- M. Iwamoto, S. Yokoo, K. Sakai and S. Kagawa, *Journal of the Chemical Society, Faraday Transactions 1: Physical Chemistry in Condensed Phases*, 1981, **77**, 1629–1638.
- M. Iwamoto, H. Furukawa, Y. Mine, F. Uemura, S.-i. Mikuriya and S. Kagawa, *Journal of the Chemical Society, Chemical Communications*, 1986, 1272–1273.
- M. Iwamoto and H. Hamada, *Catal. Today*, 1991, **10**, 57.
- C. Prestipino, G. Berlier, F. Llabrés i Xamena, G. Spoto, S. Bordiga,

- A. Zecchina, G. Turnes Palomino, T. Yamamoto and C. Lamberti, *Chemical Physics Letters*, 2002, **363**, 389–396.
- 17 S. Bordiga, C. Pazé, G. Berlier, D. Scarano, G. Spoto, A. Zecchina and C. Lamberti, *Catalysis Today*, 2001, **70**, 91–105.
- 18 C. Lamberti, A. Zecchina, E. Groppo and S. Bordiga, *Chemical Society reviews*, 2010, **39**, 4951–5001.
- 19 J. Datka, E. Kukulska-Zajac and P. Kozyra, *Journal of Molecular Structure*, 2006, **794**, 261–264.
- 20 B. Moden, P. Da Costa, D. Ki Lee and E. Iglesia, *J. Phys. Chem.*, 2002, **106**, 9633.
- 21 F. Göttl and J. Hafner, *The Journal of chemical physics*, 2012, **136**, 064502.
- 22 P. Pietrzyk, Z. Sojka, S. Dzwigaj and M. Che, *Journal of the American Chemical Society*, 2007, **129**, 14174–5.
- 23 P. Pietrzyk, W. Piskorz, Z. Sojka and E. Broclawik, *The Journal of Physical Chemistry B*, 2003, **107**, 6105–6113.
- 24 E. Broclawik, J. Datka, B. Gil, W. Piskorz and P. Kozyra, *Topics in Catalysis*, 2000, **11/12**, 335–341.
- 25 P. Rejmak, E. Broclawik, K. Góra-Marek, M. Radoń and J. Datka, *The Journal of Physical Chemistry C*, 2008, **112**, 17998–18010.
- 26 M. Davidová, D. Nachtigallová, P. Nachtigall and J. Sauer, *The Journal of Physical Chemistry B*, 2004, **108**, 13674–13682.
- 27 P. Pietrzyk and Z. Sojka, *The journal of physical chemistry. A*, 2005, **109**, 10571–81.
- 28 E. L. Uzunova, H. Mikosch and J. Hafner, *Journal of Molecular Structure: THEOCHEM*, 2009, **912**, 88–94.
- 29 E. L. Uzunova, F. Göttl, G. Kresse and J. Hafner, *The Journal of Physical Chemistry C*, 2009, **113**, 5274–5291.
- 30 R. Izquierdo, L. J. Rodríguez, R. Añez and A. Sierraalta, *Journal of Molecular Catalysis A: Chemical*, 2011, **348**, 55–62.
- 31 U. Deka, A. Juhin, E. A. Eilertsen, H. Emerich, M. A. Green, S. T. Korhonen, B. M. Weckhuysen and A. M. Beale, *The Journal of Physical Chemistry C*, 2012, **116**, 4809–4818.
- 32 N. He, H.-b. Xie and Y.-h. Ding, *Microporous and Mesoporous Materials*, 2009, **121**, 95–102.
- 33 K. Koszinowski, D. Schröder, H. Schwarz, M. C. Holthausen, J. Sauer, H. Koizumi and P. B. Armentrout, *Inorganic Chemistry*, 2002, **41**, 5882–5890.
- 34 W. F. Schneider, K. C. Hass and J. B. Adams, *Journal of Physical Chemistry B*, 1998, **5647**, 3692–3705.
- 35 N. Tajima, M. Hashimoto, F. Toyama, A. Mahmoud El-Nahas and K. Hirao, *Physical Chemistry Chemical Physics*, 1999, **1**, 3823–3830.
- 36 J. Datka and E. Kukulska-Zajac, *Studies on Surface Science and Catalysis*, 2004, 17760–17766.
- 37 M. Dewar, *Bull Soc Chim Fr*, 1951, **18**, C71–C79.
- 38 J. Chatt and L. A. Duncanson, *Journal of the Chemical Society (Resumed)*, 1953, 2939–2947.
- 39 E. Broclawik, J. Załucka, P. Kozyra, M. Mitoraj and J. Datka, *The Journal of Physical Chemistry C*, 2010, **114**, 9808–9816.
- 40 P. Kozyra, J. Załucka, M. Mitoraj, E. Broclawik and J. Datka, *Catalysis Letters*, 2008, **126**, 241–246.
- 41 P. Kozyra, M. Radon, J. Datka and E. Broclawik, *Structural Chemistry*, 2012, **23**, 1349–1356.
- 42 M. Radoń, P. Kozyra, A. Stepniowski, J. Datka and E. Broclawik, *Canadian Journal of Chemistry*, 2013, **91**, 538–543.
- 43 R. Ahlrichs, M. Bär, M. Häser, H. Horn and C. Kölmel, *Chemical Physics Letters*, 1989, **162**, 165–169.
- 44 F. Weigend and R. Ahlrichs, *Physical chemistry chemical physics: PCCP*, 2005, **7**, 3297–3305.
- 45 C. Adamo and V. Barone, *The Journal of Chemical Physics*, 1999, **110**, 6158–6170.
- 46 R. Bauernschmitt and R. Ahlrichs, *The Journal of Chemical Physics*, 1996, **104**, 9047–9052.
- 47 M. Mitoraj and A. Michalak, *Journal of molecular modeling*, 2007, **13**, 347–355.
- 48 M. Mitoraj and A. Michalak, *Organometallics*, 2007, **26**, 6576–6580.
- 49 A. Michalak, M. Mitoraj and T. Ziegler, *The journal of physical chemistry. A*, 2008, **112**, 1933–9.
- 50 M. Radoń, *Natorbs – a universal utility for calculating natural and spin density orbitals, including natural orbitals for chemical valence*, <http://www2.chemia.uj.edu.pl/~mradon/natorbs>.